The effects of level of expression of a jellyfish *Shaker* potassium channel: a positive potassium feedback mechanism

N. G. Grigoriev, J. D. Spafford and A. N. Spencer

Department of Biological Sciences, University of Alberta, Edmonton, Alberta, Canada T6G 2E9 and Bamfield Marine Station, Bamfield, British Columbia, Canada V0R 1B0

(Received 1 July 1998; accepted after revision 8 February 1999)

1. When jellyfish *Shaker* potassium channels (*jShak2*) are heterologously expressed in *Xenopus* oocytes at different levels they demonstrate density-dependent changes in electrical and kinetic properties of macroscopic currents.
2. The activation and inactivation properties of *jShak2* channels depend on the extracellular potassium concentration. In this study we present experimental data which show that expression-dependent changes in kinetic and electrical properties of *jShak2* macroscopic currents can be explained by the positive feedback effect of dynamic accumulation of K^+ in the perimembranal space.

The level of expression of *Shaker*-like potassium channels in *Xenopus* oocytes affects the electrical, kinetic and pharmacological properties of macroscopic currents. Direct protein-to-protein interaction between channels as a result of high channel density, or erroneous post-translational modification resulting from protein overproduction, have been suggested as mechanisms for expression-dependent changes in channel properties (Moran *et al.* 1992; Honore *et al.* 1992). An alternative explanation is that voltage-gated ion channels interact via the increasing concentration of ions as they accumulate in the peri-membranal micro-enviroment. For example, the intracellular accumulation of calcium ions can mediate negative feedback between L-type Ca^{2+} channels (Imredy & Yue, 1992). Here we show that expression of a *Shaker*-like channel (*jShak2*), cloned from the jellyfish *Polyorchis penicillatus*, also displays pronounced changes in properties of macroscopic currents in oocytes, which are dependent on the density of the expressed channels. We demonstrate that effluxing potassium ions feed back positively on these jellyfish *Shaker* channels by reducing the inactivation rate and increasing peak current. This mechanism accounts adequately for the changes we recorded in the properties of macroscopic currents when expressed at different levels in oocytes.

METHODS

All experimental procedures were carried out according to Canadian Council on Animal Care guidelines and all protocols were vetted by the Animal Care Committee at the University of Alberta.

Gravid female *Xenopus laevis* were anaesthetized by immersion in a 0·1% ethyl *m*-aminobenzoate (MS-222) solution for 35 min and oocytes were obtained by unilateral dorsal incision of the abdomen and removal of a lobe of an ovary. After surgery, frogs were allowed to recover for 2 h in isolation before being transferred to the post-operative tank. Frogs were carefully monitored post-operatively to ensure that they were not infected or distressed in any way. They were killed by MS-222 overdose and freezing after one procedure was performed on each side of the abdomen.

Xenopus oocytes were microinjected with various levels of RNA encoding *jShak2* (or the *jShak2*Δ2–38 mutant) channels from the hydrozoan jellyfish *Polyorchis penicillatus* and incubated for 2–3 days prior to recording (Grigoriev *et al.* 1997).

Whole-cell recordings were obtained using a CA-1 (Dagan Corporation, Minneapolis, MN, USA) amplifier in the two-electrode voltage clamp (TEVC) mode. The holding potential was −80 mV, unless otherwise stated. Special precautions were taken to avoid possible space-clamp and series resistance problems. The resistances of voltage-sensing and current-passing microelectrodes were less than 0·3 MΩ (Grigoriev *et al.* 1997): these polyacrylamide cushioned microelectrodes were positioned as far apart as possible with their tips just under the oocyte membrane. The bath clamp, a voltage-sensing mini-electrode filled with 1 M *N*-methyl-D-glucamine chloride (NMG-Cl), was positioned less than 0·2 mm from the oocyte surface. Oocytes were placed in a small, plastic V-shaped holder coated with 4% agar to prevent membrane areas contacting the plastic walls. Preliminary tests of space-clamp uniformity using oocytes expressing channels at high density (currents in the range 20–60 μA) indicated that, in most cases, voltage differences (assessed by using an additional microelectrode placed in different areas of the cytoplasm) between local and command potentials did not normally exceed 1–2% and at worst 3–5%. In general, our test data, obtained for the CA-1 amplifier, were in good agreement with results obtained for other oocyte-clamp amplifiers (P. Ruben, Utah State University, personal communication). Thus we could be fairly confident that even for currents as large as 80 μA the errors introduced by series resistance and spatial voltage non-uniformity over different membrane areas of the oocyte were not large enough to substantially affect the properties we reported at the levels of expression we used.

Cell-attached patch recordings (CAP) were performed using an Axopatch-1D amplifier (Axon Instruments) after removal of the vitelline membrane (Stühmer *et al.* 1992). A pneumatically controlled syringe pump or gravity-fed perfusion system were used for whole-cell perfusion. The standard extracellular solution (SS) contained (mM): 1 KCl, 99 NMG-Cl, 3 $MgCl_2$ and 10 Hepes adjusted to pH 7·5. Other concentrations of K^+ were made by equimolar replacement of NMG-Cl with KCl. Microinjections of KCl, TEA and CsCl were performed using a Picospritzer II (General Valve Corporation). The final intracellular concentration was estimated from an assumed dilution of 1 : 50 to 1 : 100 calculated from the cell and injected volumes. Injected volumes were estimated by measuring the diameter of a droplet injected by the micropipette into a silicone oil-filled chamber before and after each experiment. The diameter of each injected cell was measured and the volume calculated. Loose-patch recordings (LPRs) from intact oocytes were made to evaluate the spatial distribution of channels using micropipettes with openings of ~20 μm in diameter and resistances of 150–200 kΩ. Oocytes were voltage clamped using a Dagan amplifier in TEVC mode, which applies an inverted command potential to the bath while maintaining zero potential inside the oocyte. The command potential was applied simultaneously to the bath solution and the patch pipette, connected to an Axopatch-1D amplifier. This configuration allowed us to record patch and whole-cell currents simultaneously. Loose-patch pipettes have very low leakage resistances (200–300 kΩ)

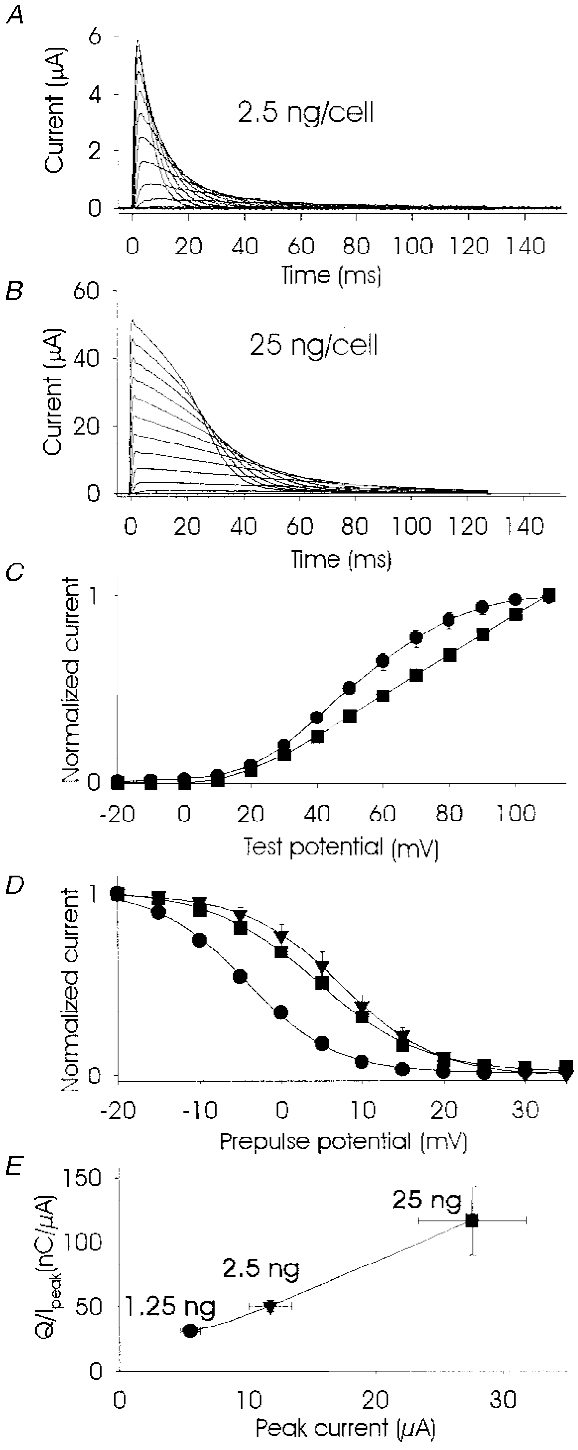

Figure 1. Effect of RNA expression level on peak current, inactivation kinetics and charge transfer of *jShak2* currents
Current traces using two-electrode voltage clamp of *jShak2* channels expressed at low (2·5 ng RNA $cell^{-1}$; *A*) and high (25 ng RNA $cell^{-1}$; *B*) levels in *Xenopus* oocytes. The stimulus protocol for *A* and *B* was 10 mV depolarizing steps from −20 to +110 mV, duration 120 ms, from a holding potential of −80 mV in standard bath solution (SS). *C* shows peak current, normalized to maximum current amplitude, *versus* test potential obtained from oocytes expressing low (2·5 ng $cell^{-1}$; ●; $n = 6$) and high (25 ng $cell^{-1}$; ■; $n = 7$) RNA levels. *D* shows steady-state inactivation curves (peak normalized current at test pulse *versus* prepulse potential) obtained from oocytes that expressed *jShak2* at high (25 ng $cell^{-1}$; ■; 1 mM $[K^+]_o$; $n = 6$) and low (2·5 ng $cell^{-1}$; ●; 1 mM $[K^+]_o$; $n = 6$) levels of RNA expression. ▼, the effect of increasing $[K^+]_o$ to 100 mM at a low level of expression ($n = 6$). A two-pulse protocol was used with a prepulse duration of 1 s from −20 to 35 mV with increments of +5 mV, 200 ms to +65 mV, separated by short 10 ms repolarizations to the holding potential of −80 mV. *E*, plot of transferred charge over a 120 ms test pulse to +65 mV *versus* peak current at different levels of *jShak2* expression. The amount of injected RNA in nanograms per cell is shown at each symbol. $n = 5$–8. Recordings were done in SS solution.

when they are pressed gently against the oocyte surface. This resistance is comparable to pipette resistance, therefore patch current is strongly contaminated with whole-cell current. To overcome this problem we used the following protocol. Initially we recorded that portion of whole-cell current produced in response to a depolarizing pulse applied to both amplifiers, passing through the pipette (I_{wc}) when it was positioned 1 mm from the oocyte surface. Then a hyperpolarizing 2 mV step was applied to the pipette alone to determine pipette resistance (R_p). After the pipette was pressed against the oocyte surface this procedure was repeated giving patch current contaminated with whole-cell current ($I_{patch,wc}$) and the resistance of the patch pipette and leakage resistance (R_{p+}). By rotation of the oocyte and re-penetration, these measurements were repeated in different regions of the oocyte surface (usually at vegetal and animal poles and the equator). Acquired current traces were used for off-line digital restoration of patch current (I_{patch}) according to the formula:

$$I_{patch} = [I_{patch,wc} - (I_{wc} R_p/R_{p+})][1 + R_p/(R_{p+1} - R_p)].$$

In the case of cell-attached patches, current density was calculated using the surface area estimated for pipettes having a similar geometry to those used in this study (Sakmann & Neher, 1983). For loose-patch recordings, membrane area was calculated by multiplying the geometrical surface area by a factor of 5, to account for membrane folding, and which was estimated from cell capacitance measurements using the ramp method. All experiments were carried out at 20 °C. Data were acquired and analysed using pCLAMP 6.0 software (Axon Instruments). Data are presented as means ± S.E.M.

RESULTS

Expression levels and current kinetics

The jellyfish channel *jShak2* showed inactivation kinetics that were strongly dependent on the level of heterologous expression in *Xenopus* oocytes. At low levels of expression (2·5 ng RNA cell^{-1}) the expressed currents inactivated rapidly (Fig. 1*A*) with a single time constant, whereas at higher levels of expression (25 ng RNA cell^{-1}) the kinetics became multiexponential (Fig. 1*B*) with slower components of inactivation predominating. Current–voltage curves at low levels of expression showed saturation, whereas at high levels of expression saturation was absent (Fig. 1*C*). The mid-point of the steady-state inactivation curve at the high level of expression was shifted rightward almost 10 mV in comparison with the low level of expression (Fig. 1*D*). It proved impractical to compare inactivation kinetics at two levels of expression based on curve fitting with a single exponential because of the complex kinetics of inactivation seen at high levels of expression. We therefore chose to compare the amount of charge (Q), normalized to peak current (I_{peak}), that was transferred at each stimulus over the same time period (Q/I_{peak}). Figure 1*E* demonstrates that both I_{peak} and transferred charge (Q/I_{peak}) increased with increasing levels of expression. It is noticeable that the variances of both I_{peak} and Q/I_{peak} were greatest at an expression level of 25 ng cell^{-1} and decreased at lower doses

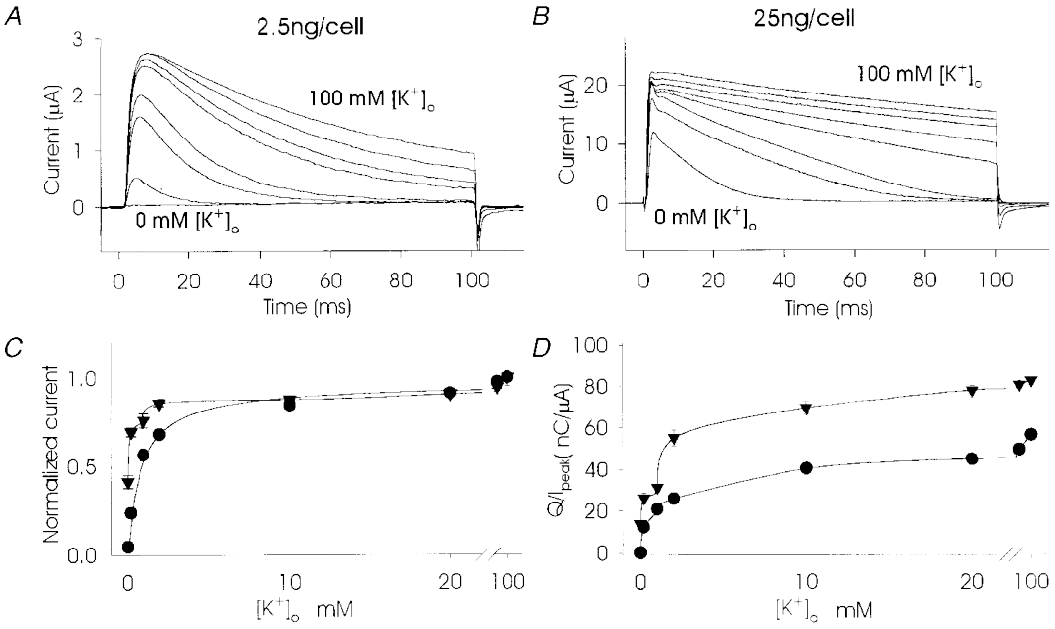

Figure 2. Sensitivity to $[K^+]_o$ of *jShak2* channels expressed in oocytes at low and high levels of RNA expression

A and *B* show superimposed TEVC recordings of currents in response to depolarizing steps to +65 mV in the presence of 0, 0·2, 1, 2, 10, 20, 40 and 100 mM $[K^+]_o$ at low (*A*) and high (*B*) levels of RNA expression. *C* shows peak current (normalized to peak current at 100 mM $[K^+]_o$) *versus* $[K^+]_o$ ($n = 6$) and *D* shows the transferred charge (normalized to peak current) *versus* $[K^+]_o$ in response to a 100 ms depolarizing pulse ($n = 6$). For *C* and *D* the currents passing through *jShak2* channels expressed at low (2·5 ng cell^{-1}; ●) and high (25 ng cell^{-1}; ▼) RNA levels are shown.

of injected RNA. Most of the increase in transferred charge at high levels of expression could be accounted for by a predominance of the slow components of inactivation.

Potassium sensitivity

jShak2 channels are known to be sensitive to the external potassium concentration, $[K^+]_o$ (N. G. Grigoriev, J. D. Spafford & A. N. Spencer, unpublished observation). As $[K^+]_o$ increases, more channels become available for activation and, at the same time, open channels inactivate more slowly and recover from inactivation faster. It is also interesting to note that increasing the external potassium ion concentration produced a marked rightward shift in the steady-state inactivation curve (Fig. 1*D*).

Channel sensitivity to $[K^+]_o$ was seen at both low and high levels of RNA expression. At low levels of expression (2·5 ng cell^{-1}) and in the absence of external potassium very few channels were activatable and in most cases no observable current was recorded (Fig. 2*A*). In contrast, at high levels (25 ng cell^{-1}) of expression, relatively large currents were recorded in the absence of external potassium (Fig. 2*B*). At low levels of expression the kinetics of inactivation were essentially monoexponential (Fig. 2*A*), whereas at high levels of expression a second, small and early current peak appeared, giving complex and variable inactivation kinetics (Figs 1*B* and 2*B*). A common pattern of inactivation at high levels of expression involved an initial phase of rapid inactivation followed by a second current peak which inactivated more slowly, producing an indistinct plateau that was terminated by an accelerated phase of inactivation. With a high level of expression at 0 mM $[K^+]_o$, inactivation was almost monoexponential while at intermediate concentrations of $[K^+]_o$ both fast and slow inactivating components were obvious (Fig. 2*B*). At the highest concentration of $[K^+]_o$, 100 mM, the fast inactivating component was less pronounced since it was probably masked by the slow component (Fig. 2*B*). Figure 2*C* and *D* demonstrates that the relationship between $[K^+]_o$ and both

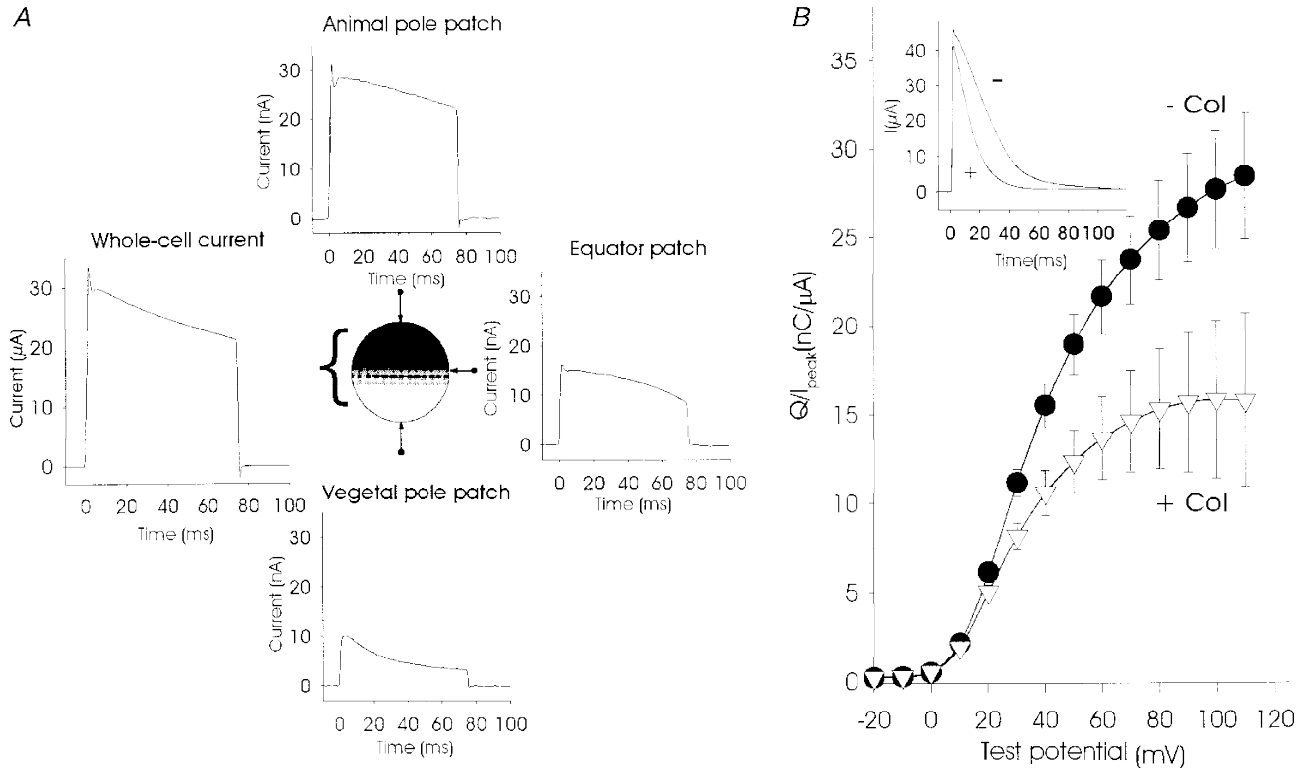

Figure 3. Spatial distribution of *jShak2* channels at a high level (25 ng cell^{-1}) of expression and the effect of colchicine treatment

The pattern of distribution of *jShak2* channels is shown in *A*, while the traces show the recorded current in response to an 80 ms depolarization step to +65 mV by using TEVC (whole-cell current) and loose-patch recording at the vegetal and animal poles and at the equator region of the same oocyte. Average peak current recorded from the animal pole was 26·5 ± 3·9 nA ($n = 12$), from the vegetal pole, 6·6 ± 1·1 nA ($n = 8$) and from the equator, 8·3 ± 2·3 nA ($n = 11$). All currents were recorded by using the same pipette with an opening diameter of 20 μm. *B* shows the effect of incubation of oocytes with 10 μM colchicine on the rate of inactivation, shown as normalized transferred charge. Oocytes were injected with 25 ng RNA cell^{-1} and incubated overnight with (▽; $n = 15$) and without (●; $n = 15$) 10 μM colchicine. Normalized transferred charge was measured in response to 100 ms depolarizing pulses from −20 to +110 mV, in steps of 10 mV, plotted against voltage. The inset shows the digitally averaged current traces obtained using a test pulse to +120 mV after overnight incubation with (+) and without (−) colchicine.

peak current and inactivation, measured as charge transfer, at low levels of expression (●) was hyperbolic. However, at a high level of expression (▼) a distinct deviation from a hyperbolic function was seen for peak current at external potassium concentrations between 0 and 2 mM (Fig. 2*C*). In addition there was a sudden increase in charge transfer that appeared between 1 and 2 mM $[K^+]_o$, producing a second hyperbolic curve after an inflexion (Fig. 2*D*). Figure 2*C* and *D* indicates that at high levels of expression the population of *jShak2* channels became heterogeneous with a sub-population exhibiting higher apparent affinity to $[K^+]_o$.

Spatial distribution of *jShak2* channels at the oocyte surface affects the kinetics of inactivation

When expressed in *Xenopus* oocytes, mammalian voltage-gated (I_{Na}, I_{Ca}) and neurotransmitter-gated channels (I_{ACh}, I_{GABA}) are not uniformly distributed since functional channels predominate at the animal pole (Peter *et al.* 1991). Since our experiments indicated a similar preferential incorporation of *jShak2* channels into the animal pole of oocytes, we suspected that the complex inactivation pattern seen in whole-cell recordings at high levels of expression resulted from this gradient of expression from the animal to the vegetal poles. It is also possible that inactivation of channels may be influenced by direct interaction between channels where they are at sufficiently high densities in the membrane. Thus, the monotonic inactivation seen at low levels of expression could indicate that a threshold density for channel–channel interaction was not achieved, so that all channels exhibited the same rates of inactivation. One of the possible mechanisms responsible for direct interaction may be interference between *N*-terminal regions of *jShak2* channels at high densities (Moran *et al.* 1992). To examine this possibility we used a mutant, *jShak2*Δ2–38, with a deletion of the first 38 amino acid residues of the N-terminus. Inactivation of wild-type *jShak2* channels expressed at low levels is predominantly of the C-type and is potassium sensitive, while N-type inactivation is not very pronounced and its presence can only be detected at high potassium concentrations or during recovery from inactivation (N. G. Grigoriev, J. D. Spafford & A. N. Spencer, unpublished observations). When we expressed *jShak2*Δ2–38 at high levels, the complex pattern of inactivation was still present, indicating that interaction involving the N-terminal region was unlikely. Using a modified version of the loose-patch recording configuration (Stühmer *et al.* 1983) we were able to establish that channel density was not uniform across the oocyte membrane both when *jShak2*Δ2–38 or the wild-type channel were expressed at high levels (Fig. 3*A*). At the vegetal pole, where channel density is lowest, the patch recordings showed comparatively rapid inactivation kinetics but as the patch was moved towards the animal pole a slowly inactivating component became increasingly more noticeable, as did an initial rapidly inactivating component (Fig. 3*A*). TEVC recordings also showed complex inactivation kinetics since the whole-cell current was representative of channels operating at a variety of densities (Fig. 3*A*).

The plasma membrane of oocytes is known to be heavily folded, forming microvilli, but the asymmetrical distribution of *jShak2* currents that we have recorded is unlikely to be associated with differences in the degree of membrane folding in different regions of the oocyte since Peter *et al.* (1991) could not detect any non-uniformity in the spatial distribution of microvilli. They also demonstrated that treating oocytes with colchicine produced a uniform distribution of heterologously expressed sodium channels without affecting the total number of activatable channels. Colchicine disrupts the cytoplasmic microtubular network,

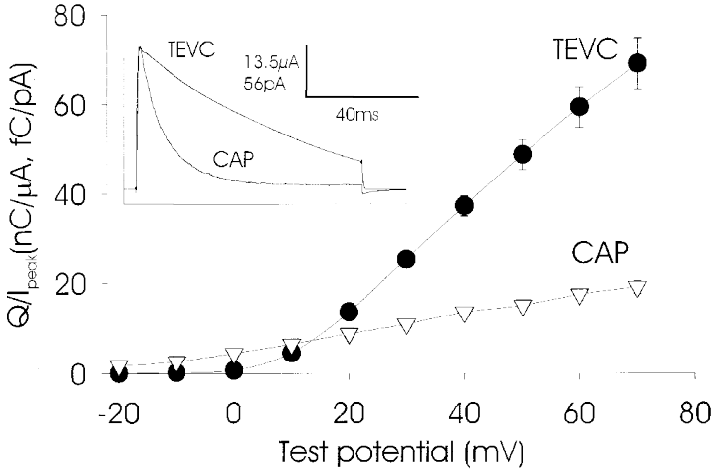

Figure 4. Inactivation properties of *jShak2* recorded using different voltage-clamp methods

Oocytes were injected with 25 ng RNA cell^{-1} and recordings made in two-electrode voltage clamp mode (TEVC; ●; $n = 5$) and in cell-attached patch mode (CAP; ▽; $n = 11$). The normalized transferred charge carried by currents was plotted against the voltage of step pulses (−20 to +70 mV in steps of 10 mV). All patch recordings were made at the animal pole. All experiments were carried out in SS. The inset shows the digitally averaged current traces obtained using a test pulse to +70 mV in TEVC and CAP modes.

which presumably interferes with transport and localization of membrane molecules (Peter *et al.* 1991).

Incubation of cells with 10 μM colchicine did not affect the number of expressed *jShak2* channels but did alter inactivation profiles (Fig. 3*B*, inset). The amplitude of the current produced by depolarizing pulses from −80 to +110 mV for control cells was 46·6 ± 3 μA ($n = 15$), and for cells incubated with colchicine this value was 42·2 ± 5 μA ($n = 15$, $P = 0{\cdot}455$). The differences seen in the inactivation parameters were reflected in the amount of normalized transferred charge (Fig. 3*B*); for control cells this value was 28·4 ± 3·53 nC μA^{-1} ($n = 15$) and for cells incubated with colchicine it was 15·8 ± 1·43 nC μA^{-1} ($n = 15$; $P = 0{\cdot}003$). Experiments using loose-patch recording (data not shown) confirmed that channels were distributed uniformly over the surface of oocytes treated with colchicine, showing that changes in inactivation properties of channels expressed at high levels are related to channel density and not to an overall high level of expression of channels.

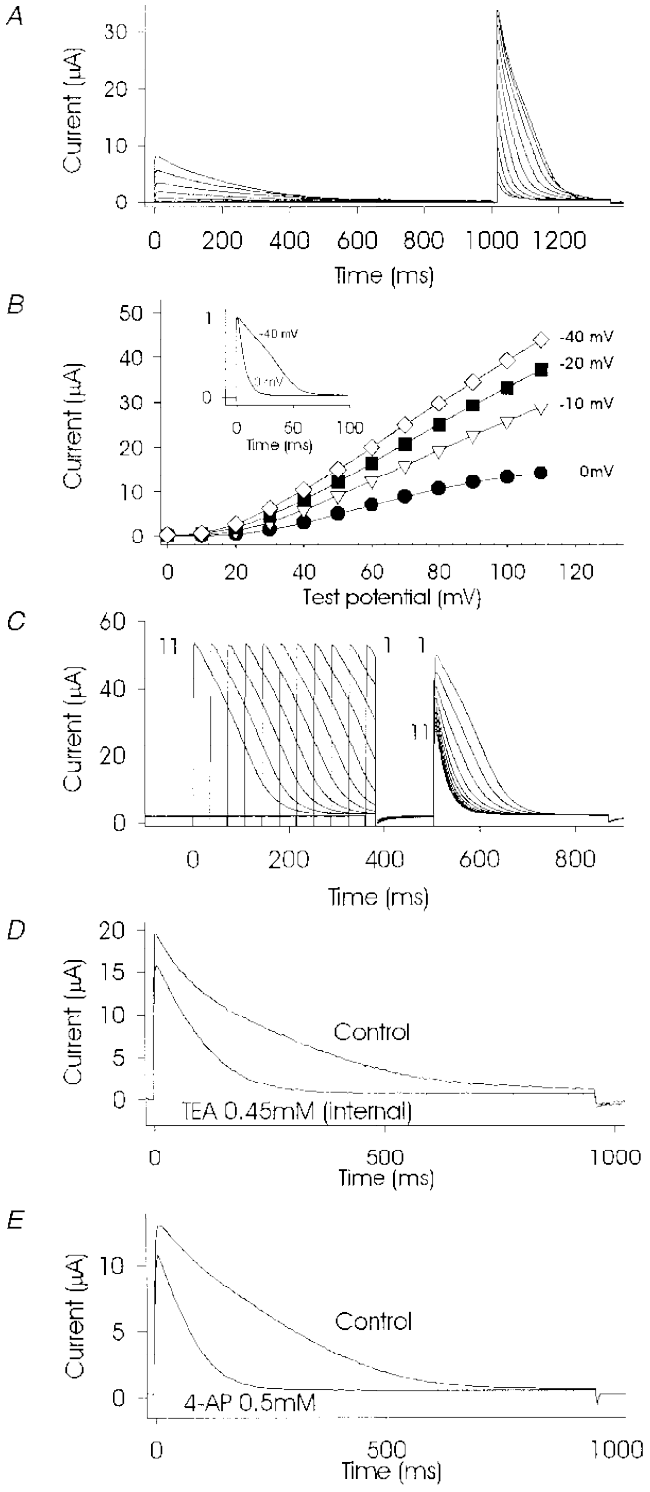

Figure 5. Treatments that reduce the number of activatable channels result in reduced peak current and faster inactivation

Partial inactivation produced by a 1 s prepulse (same protocol as for Fig. 1*D*) resulted in faster inactivation kinetics at the second, test pulse (*A*). Maintaining a holding potential at more depolarized levels (*B*) resulted in reduced peak current (graph) and faster inactivation (inset). The graph in *B* shows peak current–voltage curves obtained from one oocyte using steps of 10 mV from 0 to +110 mV. The level of the holding potential is shown beside each plot. The data points on the plots for 0 mV and −40 mV correspond to the scaled current traces (inset). *C* shows that partial inactivation due to increases in prepulse duration increased the rate of inactivation to a second, test pulse. Currents evoked by a test pulse from −80 to +85 mV, duration 360 ms, and preceded by a conditioning pulse from −80 to +85 mV of variable duration from 24 ms (pulse 1) to 384 ms (pulse 11) in steps of 26 ms are shown superimposed. Intracellular microinjection of 0·45 mM TEA (*D*), or extracellular perfusion with 0·5 mM 4-AP (*E*) also produced changes in the rate of inactivation as a result of partial channel blockade. All recordings were by TEVC from oocytes injected with 25 ng RNA cell^{-1} in SS.

Conversion from slowly to rapidly inactivating currents at high levels of expression

As described previously, high levels of expression, using the whole-cell recording configuration, produced large currents that inactivated slowly (Fig. 4, inset). However, when recordings were made from the same oocytes using the cell-attached patch configuration, the currents inactivated far more rapidly with monoexponential kinetics. This difference in inactivation kinetics between whole-cell and patch recordings was seen at all voltages above activation threshold (Fig. 4). Saturation of current–voltage curves was also seen for recordings from patches but not for whole-cell currents (data not shown). We believe that the observed kinetic discrepancy between currents recorded in whole-cell and cell-attached configurations may be explained by the accumulation of potassium, especially during repetitive activation, in the restricted spaces between the microvilli. The negative pressure created during patch formation would flatten the membrane and reduce the build-up of effluxing potassium ions in the vicinity of potassium channels which, in turn, would increase the rate of inactivation. Substantial accumulation of potassium ions effluxing through voltage-gated potassium channels in the space between the axonal membrane and Schwann cells has been reported for squid (*Loligo*) and polychaete (*Myxicola*) giant axons (Frankenhaeuser & Hodgkin, 1956; Moran *et al.* 1985).

At high levels of expression, when slow inactivation predominates, various treatments that reduced the number of activatable channels resulted in faster kinetics of inactivation. The slowly inactivating mode could be converted to a rapidly inactivating mode using the following stimulation protocols: application of conditioning prepulses (Fig. 5*A*), maintaining the holding membrane potential at a more depolarized level prior to the test pulse (Fig. 5*B*) and increasing the duration of prepulses (Fig. 5*C*). The increase in inactivation speed was associated with a switch from a mostly linear function of the current–voltage curve at a holding potential of −40 mV to a sigmoidal function at a holding potential of 0 mV (Fig. 5*B*). Partial blockage of channels by intracellular administration of tetraethylammonium (TEA), microinjected at a final concentration of 0·45 mM, also caused accelerated inactivation (Fig. 5*D*). This drug cannot be used extracellularly because it prevents inactivation by interacting with the C-type inactivating mechanism located at the channel mouth (N. G. Grigoriev, J. D. Spafford & A. N. Spencer, unpublished observations; Grissmer & Cahalan, 1989). Application of external 4-aminopyridine (4-AP) at 0·5 mM also led to an increase in the inactivation rate concomitant with partial channel block (Fig. 5*E*). The rate of inactivation was also increased after partial block of the current by intracellular administration of caesium ions (data not shown).

Increase of $[K^+]_i$ affects the inactivation rate

Increasing the intracellular potassium concentration by microinjection of potassium chloride increased the peak current amplitude with an associated slowing of inactivation, as shown in Fig. 6. This decrease in the inactivation rate could only be seen for whole-cell recordings. Control experiments were conducted by using inside-out patch recordings and altering $[K^+]_i$ within the range 100–160 mM. These recordings did not show any changes in inactivation kinetics (data not shown). Control microinjections of NaCl at the same final concentrations did not affect the current amplitude or inactivation kinetics.

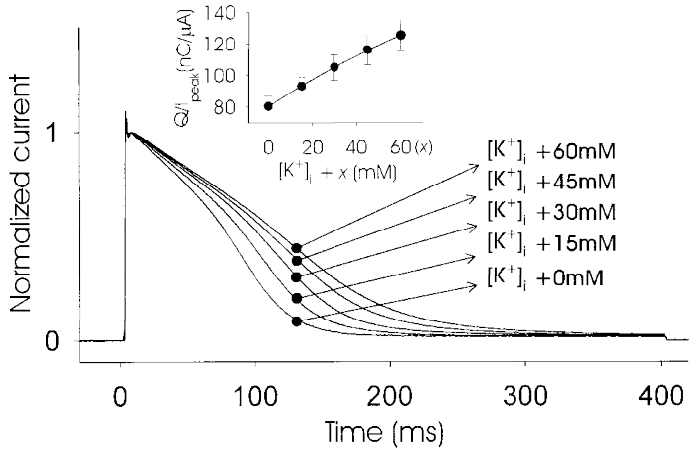

Figure 6. Increases in $[K^+]_i$ as a result of microinjection with KCl produced decreases in the inactivation rate

Oocytes expressing *jShak2* at a high level (25 ng cell^{-1}) were microinjected four times consecutively with equal aliquots of KCl to the final cytoplasmic concentrations of K^+ indicated for each current trace, which were the unknown intracellular concentration plus the added concentration (x). Currents were recorded by TEVC in response to a depolarizing pulse of +65 mV, 400 ms duration, scaled and superimposed. The inset shows a plot of normalized transferred charge *versus* $[K^+]_i + x$ ($n = 3$). Recordings were made in SS.

DISCUSSION

It is known that the level of expression of some *Shaker* potassium channels in *Xenopus* oocytes can affect the kinetics of inactivation and other channel properties. Such alterations in channel function at high levels of channel expression have been explained on the basis of protein–protein interactions due to molecular crowding or because of faulty post-translational modification due to protein overproduction (Moran *et al.* 1992; Honore *et al.* 1992). Our data do not support either of these hypotheses, but they can be explained by the sensitivity of *jShak2* channels to potassium accumulating in the extracellular micro-environment of dense channel populations.

It is known that diffusion of small molecules to or away from the oocyte plasma membrane is severely restricted by the presence of the vitelline membrane and the microvillous surface (Niu *et al.* 1996). We assume that in cell-attached macropatches the oocyte microvilli are unfolded, thereby improving the diffusion path for potassium ions and reducing the accumulation of K^+ in intermicrovillar space during synchronous channel activation. Thus, it is the accumulation of $[K^+]_o$ in intermicrovillar space that provides positive feedback on potassium-sensitive channels. At low channel densities, cross-talk between neighbouring channels via effluxing K^+ is not pronounced and total oocyte currents inactivate monotonically. However, at high channel densities such potassium cross-talk becomes significant, resulting in slower inactivation in regions of the oocyte, specifically the animal pole, where channel densities are especially high. Therefore inactivation of the total potassium current in oocytes at high levels of expression occurs with multiple time constants, reflecting the relative amount of potassium feedback in different regions of the oocyte. Potassium cross-talk in populations of *jShak2* channels could be reduced by any treatment which decreased the number of activatable channels, such as inactivation of channels or partial pharmacological blockade. Restricting potassium cross-talk between neighbouring channels by increasing the average distance between activatable channels may prevent this chain reaction occurring, and may be likened to the insertion of control rods in a nuclear reactor. A similar mechanism of ionic cross-talk has been reported for L-type calcium channels, but in that case the feedback was shown to be negative (Imredy & Yue, 1992).

The absence of current saturation at high levels of expression, as well as the appearance of a late peak during repetitive channel activation, can also be explained by peri-membranal potassium accumulation. During a step protocol each consecutive depolarization recruits more channels into an activatable pool using this chain reaction mechanism and the addition of activatable channels into the pool prevents saturation of current–voltage curves, at least within the tested range of voltage commands. A rightward shift of steady-state inactivation curves can thus be explained by the accumulation of potassium due to either high channel density or elevation of $[K^+]_o$.

Peak current density at the animal pole for the highest level of expression, in response to a depolarizing pulse from −80 to +65 mV, was estimated as 50–70 pA μm^{-2} (or 18–23 channels μm^{-2} for measured single *jShak2* channel conductance $17{\cdot}6 \pm 1{\cdot}6$ pS ($n = 6$)) from loose-patch and cell-attached recordings. The rate of potassium accumulation in the intermicrovillar space formed by four microvilli 1 μm apart over 1 ms can be estimated using the equation $C = 4I(t/F)$, where t is the time interval, I is the current density and F is the Faraday constant ($9{\cdot}648 \times 10^4$ C mol^{-1}). This calculation, which ignores diffusion of potassium out of the intermicrovillar space, gives a rate of potassium accumulation of approximately 2–3 mM ms^{-1}, which within the first few milliseconds after *jShak2* channels are activated could produce an extracellular potassium concentration tens of micromolar higher. Such an increase in $[K^+]_o$ will cause a decrease in the rate of inactivation of channels that become open by depolarization. We estimate that $[K^+]_o$ can dynamically reach 30–100 mM based on measurement of the rate of the slowest component of inactivation for currents at high levels of *jShak2* expression and the rate of inactivation for currents recorded at low levels of *jShak2* expression at different potassium concentrations. It is of interest that potassium accumulation in the periaxonal space of voltage-clamped *Myxicola* giant axon during activation of endogenous delayed rectifier current can reach as high as 60 mM in response to a 10 ms depolarizing pulse (Moran *et al.* 1985).

Electrochemical diffusion creates a decreasing potassium concentration gradient from the bottom to the apex of the microvilli, where potassium ions are diffusing into a large extracellular volume. It is possible that the fast-inactivating component of the whole-cell current at high expression levels is produced by channels at the apex of the microvilli since they will experience relatively little potassium accumulation and cross-talk, thereby inactivating rapidly. The observed increase in the apparent affinity of *jShak2* channels to $[K^+]_o$ at high channel density can also be explained by this chain-reaction mechanism. Thus, in circumstances where there is restricted accumulation of K^+, such as at low channel density or after unfolding of the oocyte membrane, no appreciable current flows at low $[K^+]_o$, until a 'critical mass' of channels is activated and the chain reaction can proceed.

It is important to note that the potassium channel densities we calculated are within the physiological range (10–1000 channels μm^{-2}) previously reported (Hille, 1992). The concentration of potassium ions in intercellular space as a result of electrical activity in the CNS of mammals can reach several millimolar in spite of the buffering properties of glial cells (Hounsgaard & Nicholson, 1983). Effluxing K^+ has been reported to cause depolarization of adjacent giant interneurones in the cockroach on a spike-by-spike basis (Yarom & Spira, 1982), and to modulate transmitter release at synapses (Weight & Erulkar, 1976). In contrast to the situation described above for the cockroach it appears that

some cells in both jellyfish and mammals (N. G. Grigoriev, J. D. Spafford & A. N. Spencer, unpublished results; Pardo *et al.* 1992) are able to counteract this depolarizing effect of increasing external [K^+] by employing a positive feedback mechanism whereby increasing K^+ accumulation increases potassium current, thereby counteracting the direct depolarizing effect of a shift in the equilibrium potential. Thus, the mechanism of positive feedback regulation of potassium channels may preserve action potential shape or other excitability properties, in spite of different extracellular K^+ regimes that arise due to variability in the surrounding diffusional barriers.

Frankenhaeuser, B. & Hodgkin, A. L. (1956). The after-effects of impulses in the giant nerve fibers of *Loligo*. *Journal of Physiology* **131**, 341–376.

Grigoriev, N. G., Spafford, D. J., Gallin, W. & Spencer A. N. (1997). Voltage sensing in jellyfish *Shaker* K^+ channels. *Journal of Experimental Biology* **200**, 2919–2926.

Grissmer, S. & Cahalan, M. (1989). TEA prevents inactivation while blocking open K^+ channels in human T-lymphocytes. *Biophysical Journal* **55**, 203–206.

Hille, B. (1992). *Ionic Channels of Excitable Membranes*, 2nd edn. Sinauer Associates, Sunderland, MA, USA.

Honore, E., Attali, B., Romey, G., Lesage, F., Barchanin, J. & Lazdunski, M. (1992). Different types of K^+ current are generated by different levels of a single mRNA. *EMBO Journal* **11**, 2465–2471.

Hounsgaard, J. & Nicholson, C. (1983). Potassium accumulation around individual Purkinje cells in cerebellar slices from the guinea-pig. *Journal of Physiology* **340**, 359–388.

Imredy, J. P. & Yue, D. T. (1992). Submicroscopic Ca^{2+} diffusion mediates inhibitory coupling between individual Ca^{2+} channels. *Neuron* **9**, 197–207.

Moran, N., Levitan E., Palti Y., Roslansky P. & Adelman W. J. Jr (1985). Significant potassium ion accumulation at the external surface of *Myxicola* giant axons. *Biochimica et Biophysica Acta* **813**, 213–220.

Moran, O., Schreibmayer, W., Weigl, L., Dascal, N. & Lotan, I. (1992). Level of expression control modes of gating of a K^+ channel. *Federation of European Biochemical Societies Letters* **302**, 21–25.

Niu, L., Vazquez, R. W., Nagel, G., Friedrich, T., Bamberg, E., Oswald, R. E. & Hess, G. P. (1996). Rapid chemical kinetic techniques for investigations of neurotransmitter receptors expressed in *Xenopus* oocytes. *Proceedings of the National Academy of Sciences of the USA* **93**, 12964–12968.

Pardo, A., Heinemann, S. H., Terlau, H., Ludewig, U., Lorra, C., Pongs, O. & Stümer, W. (1992). Extracellular K^+ specifically modulates a rat brain K^+ channel. *Proceedings of the National Academy of Sciences of the USA* **89**, 2466–2470.

Peter, A. B., Schittny, C., Niggli, V., Reuter, H. & Sigel, E. (1991). The polarized distribution of poly(A)-mRNA-induced functional ion channels in the *Xenopus* oocyte plasma membrane is prevented by anticytoskeletal drugs. *Journal of Cell Biology* **114**, 455–464.

Sakmann, B. & Neher, E. (1983). Geometric parameters of pipettes and membrane patches. In *Single Channel Recording*, ed. Sakmann, B. & Neher, E., pp. 37–52. Plenum Press, New York.

Stühmer, W., Roberts, W. M. & Almers, W. (1983). The loose patch clamp. In *Single Channel Recording*, ed. Sakmann, B. & Neher, E., pp. 123–132. Plenum Press, New York.

Stühmer, W., Terlau, H. & Heinemann, S. H. (1992). *Xenopus* oocytes for two-electrode and patch clamp recording. In *Practical Electrophysiological Methods*, ed. Grantyn, R. & Kettenmann, H., pp. 121–129. Wiley-Liss, New York.

Weight, F. & Erulkar, S. (1976). Modulation of synaptic transmitter release by repetitive postsynaptic action potentials. *Science* **193**, 1023–1025.

Yarom, Y. & Spira, M. (1982). Extracellular potassium ions mediate specific neuronal interaction. *Science* **216**, 80–82.

Acknowledgements

We thank the Bamfield Marine Station for providing excellent facilities. We are very grateful to Dr Charles Nicholson for advice and stimulating discussions. Dr Peter Ruben provided invaluable help with discussions on the limitations of two-electrode voltage clamp. J.D.S. was supported by an AHFMR studentship. Partial salary support for N.G.G. was provided by the Western Canadian Universities Marine Biological Society. This work was supported by a Natural Sciences and Engineering Research Council research grant to A.N.S.

Corresponding author

A. N. Spencer: Bamfield Marine Station, Bamfield, BC, Canada V0R 1B0.

Email: aspencer@bms.bc.ca